Structured singular value analysis for spintronics network information transfer control

E. Jonckheere, *Life Fellow, IEEE*, S. Schirmer, *Member, IEEE*, and F. Langbein, *Member, IEEE*

***Abstract*—Control laws for selective transfer of information encoded in excitations of a quantum network, based on shaping the energy landscape using time-invariant, spatially-varying bias fields, can be successfully designed using numerical optimization. Such control laws, already departing from classicality by replacing closed-loop asymptotic stability with alternative notions of localization, have the intriguing property that for all practical purposes they achieve the upper bound on the fidelity, yet the (logarithmic) sensitivity of the fidelity to such structured perturbation as spin coupling errors and bias field leakages is nearly vanishing. Here, these differential sensitivity results are extended to large structured variations using μ-design tools to reveal a crossover region in the space of controllers where objectives usually thought to be conflicting are actually concordant.**

I. Introduction

Spintronics networks [6], [7] are characterized by their unique property that information is encoded in spin excitation (understood as "spin up"), so that information transfer is mediated through spin coupling and occurs without charge movement. This offers more efficient information transfer than in devices that move charges, as heat dissipation is not a limiting factor. Excitation transport could occur through intrinsic spin dynamics, but with poor fidelity. Here, fidelity is understood as the overlap, in the sense of the absolute value of the inner product, between some desired wave function encoding a specific spin "up" and the actual terminal wave function. The point that is demonstrated here is that, despite *large* uncertainties, fidelity can be brought very near to its upper bound of 1 by means of controls taking the form of localized bias magnetic fields. This approach contrasts with another approach based on engineering the couplings. Whatever the approach, the technological challenges to be overcome are still significant. In particular, the bias magnetic fields can only be focused with limited resolution and the couplings can only be engineered with limited precision. For this reason, it is essential to assess how sensitive, *how robust,* such control schemes are against coupling and field focusing errors.

As observed in [23], the static bias magnetic field controllers that nearly achieve the fidelity upper bound have nearly vanishing (logarithmic) sensitivity to model uncertainties. This is a puzzling observation given that traditionally control predicts that one cannot simultaneously achieve small logarithmic sensitivity to uncertain parameters and small error, here defined as the departure from the fidelity upper bound. This puzzle, explained in [15], already points to quantum control deviating from classical control, in that the latter requires a physical measurement feedback process whereas the former can be accomplished by field mediation.

Here, we bring one more component to this broader study: robustness against *large* rather than differential uncertainties using μ-analysis of modern robust multivariable theory [24]. By the same token, the μ-analysis also reveals robustness against initial state preparation error. Both traditional sensitivity and μ-function are consistent in that they both define a crossover region where controllers start losing their fidelity with accrued sensitivity, while in the same region the μ-increases. These observations reinforce the earlier conclusions of [23].

E. J. is with the Department of Electrical Engineering, University of Southern California, Los Angeles, CA 90089, jonckhee@usc.edu.

S. Schirmer is with the College os Science, Swansea Univesity, Swansea, Wales, UK, s.schirmer@swansea.ac.uk.

F. Langbein is with the School of Computer Science & Informatics, Cardiff University, Cardiff, Wales, UK, F.C.Langbein@cs.cardiff.ac.uk.

Manuscript received October 2016; revised ???.

A. Outline

The basic concepts associated with the control of spintronics networks for *time-domain* high fidelity information transfer are reviewed in Section II. As a preview to the robustness issue, in Section III, we explore the (differential) sensitivity of the achieved fidelity to coupling uncertainties and bias field leakage errors. "Sensitivity" means that the perturbations are infinitesimal. From this point on, the perturbations become larger and we examine "robustness." In Section IV, the perturbation is formulated as a diagonally structured feedback. In Section IV-D, the ground work is prepared for the reformulation of the time-domain figure of merit to its frequency-domain counterpart. In Section V, the μ-analysis is set up, and in Section VI, the μ-analysis is performed on an 11-spin ring, providing controllers maintaining good fidelity under large perturbations.

II. Basic concepts

A. Information transfer control

We consider homogeneous chains or rings of N spins with XX or Heisenberg couplings [11], [12], [13], [14], [15], [20]. Each spin can be up $|\uparrow\rangle$ or down $|\downarrow\rangle$. Within the Hilbert space C^{2^N} of this network, we define the single excitation subspace as the span of $|\downarrow\rangle^{\otimes(k-1)}\otimes|\uparrow\rangle\otimes|\downarrow\rangle^{\otimes(N-k)}$, where k runs from 1 to N. Intuitively, this is the subspace where exactly one spin is "up." This subspace is invariant under the motion and in this subspace the Hamiltonian takes the matrix representation

$$H=\begin{pmatrix} 0 & 1 & 0 & \dots & 0 & h_{1,N} \\ 1 & 0 & 1 & & 0 & 0 \\ 0 & 1 & 0 & & 0 & 0 \\ \vdots & & \ddots & \ddots & \ddots & \vdots \\ 0 & 0 & 0 & & 0 & 1 \\ h_{N,1} & 0 & 0 & \dots & 1 & 0 \end{pmatrix}, \tag{1}$$

where $h_{1,N}=h_{N,1}=0$ for XX-chains and $h_{1,N}=h_{N,1}=1$ for XX-rings. For Heisenberg XXX-couplings, an identity matrix should be added to (1). The Hilbert space of the system now is $\mathbb{C}^N$ with natural basis $\{e_k\}_{k=1}^N$. In this single excitation subspace, $|\Psi\rangle=e_k$ denotes the state where the excitation (the only "spin up") is on spin #k. To achieve the objective of *transporting* the excitation from an initial wave function state $|\mathrm{IN}\rangle=|\Psi(0)\rangle$, localized at a spin, to a terminal state $|\mathrm{OUT}\rangle=|\Psi(t_f)\rangle$, localized at another spin, spatially distributed but time-invariant bias fields $\{D_i : i=1,...,N\}$ are applied to the respective spins. Defining $D=\mathrm{diag}\{D_i : i=1,...,N\}$ results in the controlled Hamiltonian $H+D$. With this Hamiltonian, and under the assumption that the system is isolated from its environment, the evolution is described by Schrödinger's

equation $|\dot{\Psi}(t)\rangle = -\imath(H+D)|\Psi(t)\rangle$. Schrödinger's equation can be broken down, a bit artificially, into a classical state space equation

$$|\dot{\Psi}(t)\rangle = -\imath H|\Psi(t)\rangle + u(t), \tag{2}$$

driven by the control

$$u(t) = -\imath D|\Psi(t)\rangle. \tag{3}$$

Eqs. (2)-(3) formulate the transport problem in the set-up of control theory, with the drawback that the "feedback" (3) is only "virtual."

In [20], [23], for each $(|\mathrm{IN}\rangle, |\mathrm{OUT}\rangle)$ pair, a set of bias controllers $\{D(m)\}_{m=1}^{1000}$, where $D(m) = \mathrm{diag}(D_1(m), D_2(m), ..., D_N(m))$, was derived and the controllers were ordered by decreasing order of their squared fidelities, or probabilities of achieving successful transfer,

$$p_{t_f(m)}(|\mathrm{IN}\rangle, |\mathrm{OUT}\rangle) = \left|\left\langle \mathrm{OUT}|e^{-\imath(H+D(m))t_f(m)}|\mathrm{IN}\right\rangle\right|^2,$$

where $t_f(m)$ is the time at which the controller $D(m)$ achieves its maximum fidelity. Such fidelity or probability of successful transfer will be referred to as "instantaneous." The design was a purely numerical approach to the problem of achieving optimal fidelity

$$\max_D |\langle \mathrm{OUT}|\Psi(t_f)\rangle| \leq 1 \tag{4}$$

in a minimum amount of time t_f. The latter is motivated by the need to act faster than the decoherence. Because the landscape in which the optimization is performed is extremely challenging [20, Fig. 2], only *some* runs were successful at getting very close to the upper bound of 1, while other runs were not as successful, with the reward that this gave us controllers achieving various level of fidelity, opening the road to explore potential conflicts with other objectives such as sensitivity and robustness.

B. Quantum-classical control design discrepancies

1) Measurements or no measurements?: Eqs. (2)-(3) certainly allow us to formulate the quantum mechanical problem as a control problem, that is, a state-space equation (2) driven by a control u, itself depending linearly on the state $|\Psi\rangle$ as seen by (3). The problem is that breaking the Schrödinger equation into two parts introduces a control u that is artificial, that does not have physical existence, but that nevertheless exists mathematically. Even though there is no *physical* closed-loop backward measurement signal flow, the "virtual" feedback structure, even somewhat "hidden," has been shown to endow the system with good differential sensitivity properties relative to spin coupling uncertainties [15], [23]. This is a property certainly consistent with measurement feedback.

One of the purposes of this paper is to clarify whether those differential sensitivity properties translate to robustness under larger variations of the spin couplings.

Attempts at classifying the many quantum control laws abound, but here we will particularly retain the classification of [5], which emphasizes, as the present paper does, time-invariant spatially-distributed control. Control is defined in [5] as manipulating matter-field or field-field interactions. In this classification, our approach is rather a *field-field* interaction, or in other words our controller is *field-mediated.* The localized magnetic fields that are applied to the spins change the total energy of the system through the spin-field interaction; those magnetic fields are registered in the Hamiltonian as the additional diagonal terms of D, which alter the dynamics so to achieve a specific transport.

2) Lack of closed-loop stability: Eq. (3) is a bit misleading, as the control D is *selective,* in the sense that it depends on both $|\mathrm{IN}\rangle$ and $|\mathrm{OUT}\rangle$. This is contrary to classical tracking where the initial state is the quiescent state and the controller is designed to go to any terminal state. The selectivity implies that we need to repudiate the classical closed-loop stability. Indeed, if a controller is designed so as to achieve $|\mathrm{IN}\rangle \to |\mathrm{OUT}\rangle$, no other initial state say $|\mathrm{IN}'\rangle$ would reach $|\mathrm{OUT}\rangle$ even asymptotically; indeed, because of the unitary evolution $\|U(t_f)(|\mathrm{IN}\rangle - |\mathrm{IN}'\rangle)\| = \||\mathrm{IN}\rangle - |\mathrm{IN}'\rangle\| \neq 0$. Besides, it is obvious that the closed-loop matrix $-\imath(H+D)$ is purely oscillatory.

In physics language, even though $|\Psi(t_f)\rangle$ might get very close to $|\mathrm{OUT}\rangle$ at some specific t_f, over the larger time interval the best one can expect is to have $|\Psi(t)\rangle$ oscillate in a localized manner around $|\mathrm{OUT}\rangle$. The oscillation is "localized" in the sense that the support of the wave function is a compact neighborhood of $|\mathrm{OUT}\rangle$. This is akin to the concept of Anderson localization [1], [9], [19], except that Anderson localization is formally meant to keep an excitation localized around a spin, whereas here it is an unexpected property of the transfer controller.

C. Structured uncertainties

The objective is to examine the robustness of the D-scheme under perturbation of the 2-body interaction strengths, that is, a perturbation of the Hamiltonian matrix H that takes the form

$$\begin{aligned} &H + \Delta_H \\ &= \begin{pmatrix} 0 & 1+\delta_{12} & \dots & 0 & H_{1,N}+\delta_{1,N} \\ 1+\delta_{12} & 0 & & 0 & 0 \\ & & & & \\ 0 & 0 & & 0 & 1+\delta_{N-1,N} \\ H_{N,1}+\delta_{1,N} & 0 & & 1+\delta_{N-1,N} & 0 \end{pmatrix} \\ &= H + \sum_{k=1}^{N-1} \delta_{k,k+1} S_{k,k+1} + \delta_{1,N} S_{1,N}, \end{aligned}$$

where $S_{k,k+1}$ is the *structure* associated with the perturbation of the $(k,(k+1))$ coupling, with the convention that $\delta_{1,N} = 0$ if $h_{1,N} = 0$ (chain), and $\delta_{k,k+1}$ is the magnitude of the perturbation. Clearly, this is a *structured* perturbation, and the classical way of assessing robustness against such a structured perturbation is via the μ-analysis [16], [17], [24].

Other uncertainties to be taken into consideration are the inaccuracies in the localization of the magnetic fields implementing the biases. In this case, the Hamiltonian is perturbed as

$$H + D + \Delta_D = H + D + \sum_{k=1}^{N} \delta_{kk} S_{kk} D_k,$$

where

$$S_{kk} = \mathrm{diag}\left(0, 0, ..., 0, \frac{1}{2}, -1, \frac{1}{2}, 0, ..., 0, 0\right),$$

assuming that the bias that should nominally be applied to spin k spill over symmetrically to the nearest-neighbor spins.

III. Small perturbation sensitivity

The fundamental objective in [20], [23] was the maximization of the squared fidelity or probability, $\left|\left\langle \mathrm{OUT}|e^{-\imath(H+D(m))t_f(m)}|\mathrm{IN}\right\rangle\right|^2$, over D-structured controllers, *for the nominal model of the spin network.* This raises the question of how sensitive the squared fidelity is to network modeling errors

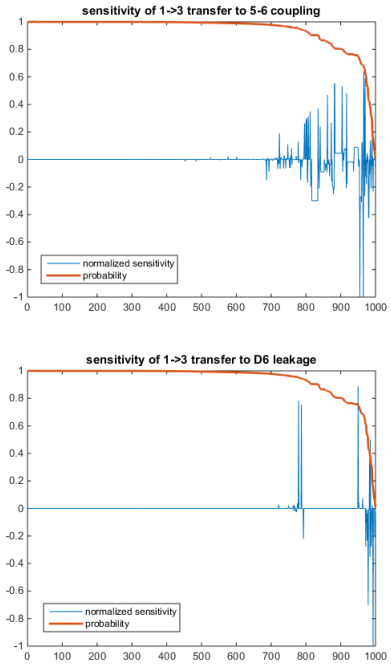

Fig. 1. Plot of instantaneous probability (squared fidelity) and sensitivity versus index m of the controllers; top: sensitivity relative to coupling uncertainty; bottom: sensitivity relative to leakage of bias field to near neighbor spins.

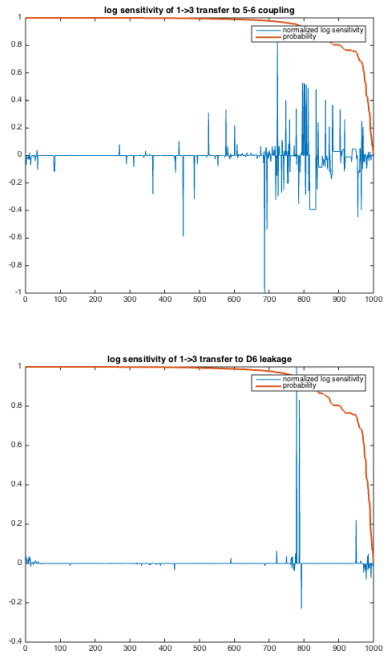

Fig. 2. Plot of instantaneous probability (fidelity squared) and logarithmic sensitivity versus index m of the controllers; top: log sensitivity relative to coupling uncertainty; bottom: log sensitivity relative to leakage of bias field to near neighbor spins.

and departure of the controller from bias fields highly localized around their respective spins:

$$\begin{aligned}\frac{\partial}{\partial\delta_{k,k+1}}\left|\left\langle \mathrm{OUT}|e^{-\imath(H+D(m)+\delta_{k,k+1}S_{k,k+1})t_f(m)}|\mathrm{IN}\right\rangle\right|^2,\\ \frac{\partial}{\partial\delta_{kk}}\left|\left\langle \mathrm{OUT}|e^{-\imath(H+D(m)+\delta_{k,k}S_{k,k}D_k(n))t_f(m)}|\mathrm{IN}\right\rangle\right|^2.\end{aligned} \tag{5}$$

Classically, one would expect the fidelity and the inverse sensitivity (a measure of "robustness") to go in opposite direction. As shown by Fig. 1, this is not the case, as the best fidelity controllers have the least sensitivity. From both plots of Fig. 1, the sensitivity deteriorates (increases) as soon as the squared fidelity begins to dip. The same pattern holds for the logarithmic sensitivity, where the expressions in Eqs. (5) are divided by the error, that is, $1-|\langle \mathrm{OUT}|\Psi(t_f(m))\rangle|^2$, as shown in Fig. 2. Both plots indicate a "crossover" region where fidelity and sensitivity begin to change markedly. One of the purposes of the paper is to show that the μ-analysis is consistent with this finding.

IV. Large diagonally-structured perturbation

A. Coupling uncertainty

Consider the closed-loop perturbed system

$$\begin{aligned}|\dot\Psi(t)\rangle = -\imath(H+D)|\Psi(t)\rangle - \imath\sum_{k=1}^{N-1}\delta_{k,k+1}S_{k,k+1}|\Psi(t)\rangle\\ -\imath\delta_{1,N}S_{1,N}|\Psi(t)\rangle.\end{aligned} \tag{6}$$

The objective of maximization of $|\langle \mathrm{OUT}|\Psi(t)\rangle|$ is easily seen to be equivalent to minimization of $|\langle \mathrm{OUT}^\perp|\Psi(t)\rangle|$, where $|\mathrm{OUT}^\perp\rangle$ denotes a basis of the orthogonal complement of $|\mathrm{OUT}\rangle$. The output signal that usually assesses the performance of a control system can hence be defined rather classically as

$$z(t) = \langle \mathrm{OUT}^\perp|\Psi(t)\rangle = C\Psi(t),$$

where the rows of the matrix C form a basis of $|\mathrm{OUT}\rangle^\perp$. Contrary to the classical control paradigm where a disturbance signal drives the system, here the system responds to an initial state $|\mathrm{IN}\rangle$. With the time-invariant bias matrix D, the output $|\Psi(t)\rangle$ and the control $u(t)$ can be "virtually" connected via $-\imath D$, as shown in Fig. 3.

1) One single coupling uncertainty: Computation of robustness margin against structured uncertainties relies on extracting the uncertain parameters from the perturbed system and displaying them as a diagonally structured "fictitious" feedback from an artificially defined output ζ to an artificially defined input v both defined on the unperturbed system, as shown in Fig. 3. To unravel this structure, we use the matrix inversion lemma:

$$\begin{aligned}(sI+\imath H+\imath\delta_{k,k+1}S_{k,k+1})^{-1} =\\ (sI+\imath H)^{-1}\\ -\ (sI+\imath H)^{-1}\delta_{k,k+1}I\left(I+\imath S_{k,k+1}(sI+\imath H)^{-1}\delta_{k,k+1}I\right)^{-1}\\ \times\imath S_{k,k+1}(sI+\imath H)^{-1}.\end{aligned}$$

Observe that the uncertainty $\delta_{k,k+1}$ must be multiplied by the identity $I_{N\times N}$ to safeguard compatibility among the sizes of the various matrices, something that unfortunately creates a significant curse of dimensionality. Now, write the open-loop unperturbed plant as

$$\begin{pmatrix}\zeta\\ |\Psi\rangle\end{pmatrix} = \begin{pmatrix}P_{11} & P_{13}\\ P_{31} & P_{33}\end{pmatrix}\begin{pmatrix}v\\ u\end{pmatrix}.$$

A fictitious feedback Δ from ζ to v would give the transfer matrix from u to v as

$$(sI+\imath H+\imath\delta_{k,k+1}S_{k,k+1})^{-1} = P_{33}+P_{31}\Delta(I-P_{11}\Delta)^{-1}P_{13}.$$

Comparing the two expressions for the open-loop system perturbed by the fictitious feedback yields

$$\begin{pmatrix}P_{11} & P_{13}\\ P_{31} & P_{33}\end{pmatrix} = \begin{pmatrix}-\imath S_{k,k+1}(sI+\imath H)^{-1} & \imath S_{k,k+1}(sI+\imath H)^{-1}\\ -(sI+\imath H)^{-1} & (sI+\imath H)^{-1}\end{pmatrix}$$

together with

$$\Delta = \delta_{k,k+1} I_{N\times N}.$$

With P_{11}, P_{13}, P_{31} and P_{33} taken care of, it remains to define the second block row of P (output variable z) and the second block column of P (input variable $\Psi(0)$). The idea is to observe that the second and last block columns of P are the same, since u and $|\mathrm{IN}\rangle$ have exactly the same effect on the dynamics. From there on, making use of the matrix C, it is easily seen that $(P_{21}, P_{22}, P_{23}) = C(P_{31}, P_{32}, P_{33})$. Then we derive the remaining second block row and second block columns of P as

$$\begin{aligned} P_{32} &= P_{33}, \\ P_{21} &= CP_{31}, \\ P_{22} &= CP_{32}, \\ P_{23} &= P_{22}, \\ P_{12} &= P_{13}. \end{aligned}$$

Setting $\Phi := (sI + \imath H)^{-1}$ to simplify the notation, the block 3×3 plant equation of Fig. 3 becomes

$$\begin{pmatrix} \zeta \\ z \\ \Psi \end{pmatrix} \begin{pmatrix} -\imath S_{k,k+1}\Phi & \imath S_{k,k+1}\Phi & \imath S_{k,k+1}\Phi \\ -C\Phi & C\Phi & C\Phi \\ -\Phi & \Phi & \Phi \end{pmatrix} \begin{pmatrix} v \\ |\mathrm{IN}\rangle \\ u \end{pmatrix}. \tag{7}$$

2) Many uncertain couplings: To avoid clutter, we consider only two coupling uncertainties, $\delta_{k,k+1}$ and $\delta_{\ell,\ell+1}$. The general pattern of N (or $N-1$) uncertain couplings for a ring (or a chain) will clearly emerge from this simple case. It is claimed that the subset of P-equations relevant to the uncertainty feedback model is

$$\begin{pmatrix} \zeta_k \\ \zeta_\ell \\ \Psi \end{pmatrix} = \begin{pmatrix} -\imath S_{k,k+1}\Phi & -\imath S_{k,k+1}\Phi & \imath S_{k,k+1}\Phi \\ -\imath S_{\ell,\ell+1}\Phi & -\imath S_{\ell,\ell+1}\Phi & \imath S_{\ell,\ell+1}\Phi \\ -\Phi & -\Phi & \Phi \end{pmatrix} \begin{pmatrix} v_k \\ v_\ell \\ f \end{pmatrix},$$

where $f := |\mathrm{IN}\rangle + u$ is the forcing term. Using the matrix inversion lemma, it is easily seen that closing the loop $v_k = \delta_{k,k+1} I_{N\times N}\zeta_k$ yields

$$\begin{pmatrix} \zeta_\ell \\ \Psi \end{pmatrix} = \begin{pmatrix} -\imath S_{\ell,\ell+1}\Phi_k & \imath S_{\ell,\ell+1}\Phi_k \\ -\Phi_k & \Phi_k \end{pmatrix} \begin{pmatrix} v_\ell \\ f \end{pmatrix},$$

where $\Phi_k := (sI + \imath H + \imath\delta_{k,k+1}S_{k,k+1})^{-1}$. Appealing one more time to the matrix inversion lemma reveals that closing the loop $v_\ell = \delta_{\ell,\ell+1} I_{N\times N}\zeta_\ell$ yields

$$\begin{aligned} \Psi &= \left(\Phi_k^{-1} + \delta_{\ell,\ell+1}\imath S_{\ell,\ell+1}\right)^{-1} f \\ &= (sI + \imath\delta_{k,k+1}S_{k,k+1} + \imath\delta_{\ell,k+1}S_{k,k+1})^{-1} f, \end{aligned}$$

as claimed.

In this case of two uncertain couplings, the block 3×3 plant equation becomes

$$\left(\begin{array}{cc|c|c} -\imath S_{k,k+1}\Phi & -\imath S_{k,k+1}\Phi & \imath S_{k,k+1}\Phi & \imath S_{k,k+1}\Phi \\ -\imath S_{\ell,\ell+1}\Phi & -\imath S_{\ell,\ell+1}\Phi & \imath S_{\ell,\ell+1}\Phi & \imath S_{\ell,\ell+1}\Phi \\ \hline -C\Phi & -C\Phi & C\Phi & C\Phi \\ \hline -\Phi & -\Phi & \Phi & \Phi \end{array}\right).$$

B. Leakage of bias field to near-neighbor spins

In case of uncertainty on the focusing power of the bias field, restricting ourselves to the nominal bias field D_{kk} spilling over spins $k-1$ and $k+1$, the perturbed dynamics becomes

$$|\dot\Psi(t)\rangle = -\imath(H+D)|\Psi(t)\rangle - \imath\sum_{k=1}^{N}\delta_{k,k}S_{k,k}D_{kk}|\Psi(t)\rangle. \tag{8}$$

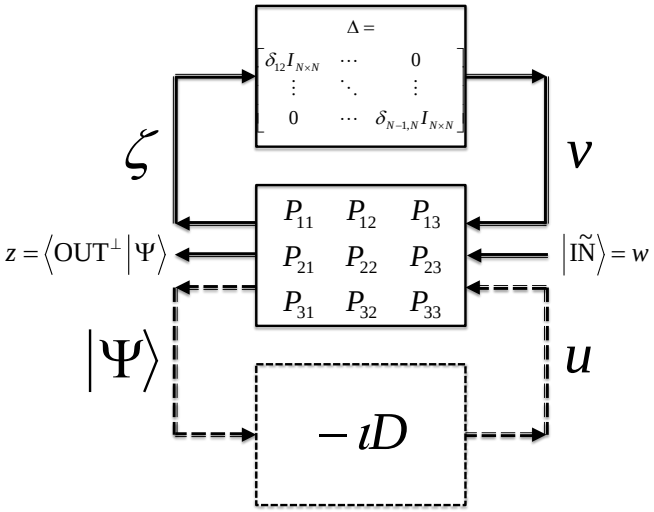

Fig. 3. Modern robust multivariable control inspired diagram showing the perturbation as a diagonally structured feedback. The dotted path from $|\Psi\rangle$ to u means that the feedback is virtual, not measurement mediated.

C. General architecture

The overall control-inspired architecture of the quantum system is shown in Fig. 3. The 3×3 system P is open-loop, unperturbed. The top feedback introduces the uncertain parameters, as explained in Sec. IV-A1. The bottom (dotted) flow is a representation of the control (2)-(3). This flowchart might give the wrong impression that there is a need to measure $|\Psi(t)\rangle$ with the potential danger of back-action of the measurement. Quite to the contrary, as already argued in Sec. II-B1, there is no measurement feedback, only a *virtual* feedback. The prepared state $|\mathrm{IN}\rangle$ is the initial condition, viewed as a disturbance input $w(t)$ to the system, modeling a constant but uncertain preparation error on the initial state. The overall system is set up in such as way as to respond to $w(t)$, as shown in Fig. 3. The output is the error $\langle\mathrm{OUT}^\perp|\Psi(t)\rangle$. Since

$$|\langle\mathrm{OUT}^\perp|\Psi(t)\rangle|^2 + |\langle\mathrm{OUT}|\Psi(t)\rangle|^2 = 1,$$

to secure a squared fidelity $|\langle\mathrm{OUT}|\Psi(t)\rangle|^2 \geq 1-\epsilon$, it suffices to take $|\langle\mathrm{OUT}^\perp|\Psi(t)\rangle|^2 \leq \epsilon$.

D. Time-domain versus frequency-domain design

The fidelity with the bias control $D(m)$ remains oscillating around the target state and the maximum fidelity is recorded at $t_f(m)$. This is of course a time-domain approach, with difficulties to be translated to the traditional frequency-response methods of modern robust multivariable control. Here we take a simplified approach to the problem by trading the maximum fidelity over time for a time-averaged fidelity. Besides, the instantaneous fidelty can never been observed, as the read-out device can only time-average over a finite window.

The question of whether this time-average can be related to the time-optimal fidelity is here justified only by a simulation study. In Fig. 4, the controllers are ordered by decreasing value of the fidelity at $t_f(m)$ and compared with an average fidelity obtained by a Lyapunov method (which correlates very well with the averaging over $2t_f(m)$). A qualitative concordance between the behavior of the mean fidelity and that of the time-optimal fidelity can be seen, confirmed by a Kendall τ of 0.3621.

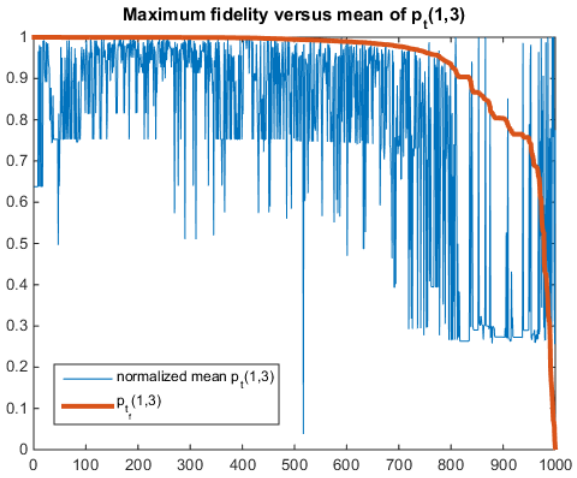

Fig. 4. Behavior of maximum squared fidelity at $t_f(m)$ versus time-averaged fidelity

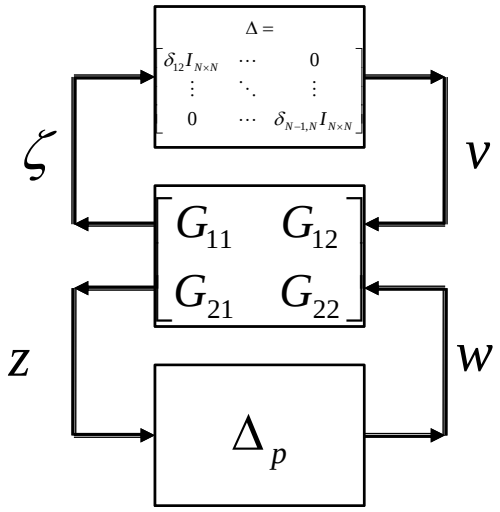

Fig. 5. Classically inspired robust performance design showing a fictitious perturbation Δ_p feedback from performance output to disturbance input

V. μ-ANALYSIS

In [20], given an $(|\mathrm{IN}\rangle, |\mathrm{OUT}\rangle)$ pair, a collection $\{D(m)\}_{m=1}^{1000}$ of diagonal matrices satisfying the transport requirement in a varying amount of time with varying degree of success was derived. The objective here is to assess the fidelity versus the μ-robustness. Classically, one would expect a trade-off between fidelity and sensitivity. However, Fig. 1 indicates that this well known fundamental limitation in its differential form does not survives the passage to the quantum world. The problem is that no matter how encouraging the near vanishing sensitivity mediated by the best fidelity controllers is, it does not answer the question of large deviation, as the sensitivity in [23] was computed for $\delta = 0$. We attempt to address this question classically using the robust performance formalism [24, Chap. 10], but we immediately have to deviate from the classical formalism on two major points:

1) There is no stability requirement. Indeed, the wave function of the physically motivated Anderson localization [1] is purely oscillatory.
2) The disturbance input $w(t)$ of Fig. 3 is not in L^2, but is a constant in time but uncertain initial preparation $|\tilde{\mathrm{IN}}\rangle$ of $|\mathrm{IN}\rangle$. In other words, using a concept developed in [2], the input is in exponential regime e^{0t}. Hence that part of the output at that exponential regime is

$$\widehat{z}(0) = C\widehat{\Psi}(0) = C\,(sI + \imath(H+D))^{-1}\big|_{s=0}\,|\tilde{\mathrm{IN}}\rangle.$$

With the convention that $w = |\tilde{\mathrm{IN}}\rangle$, this leads us to define

$$T_{zw}(s) = C(sI + \imath(H + D(|\mathrm{IN}\rangle, |\mathrm{OUT}\rangle))^{-1}\big|_{s\approx 0}$$

as the closed-loop performance indicator. Indeed, setting $\tilde{\mathrm{IN}} = \mathrm{IN} + \boldsymbol{\delta}$, we obtain for near perfect state transfer controllers $T_{zw}|\tilde{\mathrm{IN}}\rangle \approx T_{zw}\boldsymbol{\delta}$, so that $T_{zw}w$ provides the response to the preparation error amplified by the uncertainty lumped in T_{zw}.

We proceed from Fig. 3 and absorb the controller in the plant to come up with

$$\begin{pmatrix} \zeta \\ z \end{pmatrix} = \begin{pmatrix} G_{11} & G_{12} \\ G_{21} & G_{22} \end{pmatrix} \begin{pmatrix} v \\ w \end{pmatrix}, \tag{9}$$

where

$$\begin{aligned} G_{11} &= P_{11} - P_{13}\imath D(I + P_{33}\imath D)^{-1}P_{31}, \\ G_{12} &= P_{12} - P_{13}\imath D(I + P_{33}\imath D)^{-1}P_{32}, \\ G_{21} &= P_{21} - P_{23}\imath D(I + P_{33}\imath D)^{-1}P_{31}, \\ G_{22} &= P_{22} - P_{23}\imath D(I + P_{33}\imath D)^{-1}P_{32}, \end{aligned} \tag{10}$$

as shown in Fig. 5. From Eq. (9), it is easily seen that the performance can be assessed via

$$T_{zw} = G_{22} + G_{12}\Delta\,(I - G_{11}\Delta)^{-1}\,G_{12}.$$

The μ-design specification (see, e.g., [24, Th. 10.8]) is formulated as

$$\|T_{zw}\| \le \beta \text{ for all } \|\Delta\| < 1/\beta. \tag{11}$$

As β decreases, observe that the response to the initial preparation error decreases while this decrease occurs for larger uncertainties. Hence β is a robustness measure. As we are soon to show, β can be evaluated via the μ-function.

The specification (11) can be rewritten as $\det(I - T_{zw}\Delta_p) \neq 0$ for all fictitious perturbations $\|\Delta_p\| < 1/\beta$. The fictitious perturbation can be reinterpreted as a feedback from z to w and the specification $\|T_{zw}\| \le \beta$ for all $\|\Delta_p\| < 1/\beta$ means that $\det(I - T_{zw}\Delta_p) \neq 0$. The difficulty is that T_{zw} depends on another Δ. This difficulty can be overcome by observing that

$$\det(I - G_{11}\Delta)\det\,(I - T_{zw}\Delta_p) = \det(I - G\boldsymbol{\Delta}), \tag{12}$$

where $\boldsymbol{\Delta}$ is the augmented structured perturbation

$$\boldsymbol{\Delta} = \begin{pmatrix} \Delta & 0 \\ 0 & \Delta_p \end{pmatrix}, \quad \|\boldsymbol{\Delta}\| < 1/\beta.$$

$\boldsymbol{\Delta}$ is structured in two different ways: first of all it has block diagonal structure and secondly Δ is diagonal. Ideally, the structure imposed upon Δ_p is that its column space should reproduce the space of initial preparations of $|\Psi(0)\rangle$.

In view of (12), the condition for robust performance now becomes $\det(I - G\boldsymbol{\Delta}) \neq 0$ for all structured $\|\boldsymbol{\Delta}\| < 1/\beta$. It is well known (see, e.g., [24, Th. 10.8]) that the latter is equivalent to

$$\mu_{\mathcal{D}}(G) \le \beta,$$

where $\mu_{\mathcal{D}}$ denotes the μ-function, or structured singular value, relative to the set of matrices $\mathcal{D}$ structured as $\mathbf{\Delta}$. Specifically,

$$\mu_{\mathcal{D}}(G) = \frac{1}{\min\{\|\mathbf{\Delta}\| : \mathbf{\Delta} \in \mathcal{D}, \det(I - G\mathbf{\Delta}) = 0\}}.$$

Observe that the upper bound β can be interpreted as *some* sensitivity of the performance relative to the structured perturbation. Indeed, if β is small, $\|T_{zw}\|$ remains small for large Δ's and hence the sensitivity is small. An exact relationship, if any, between β and the sensitivity in the sense of Sec. IV-D, Eq. (5), is hard to come by; however, the next section will provide an illustration that such a relationship is plausible.

VI. 11-spin ring simulation example

Here we give an example illustrating that the unconventional behavior of the fidelity versus spin coupling sensitivity depicted in Figures 1-2 survives the double passage (i) from instantaneous to time-averaged performance and (ii) from differential sensitivity to robustness against larger variations—and initial preparation errors.

We take an 11-ring with nominally uniform coupling strengths between near neighbor spins, but subject to a 5-6 uncertain coupling, under $|1\rangle \rightarrow |3\rangle$ transfer. For this transfer, we have the controllers $\{D(m)\}_{m=1}^{1000}$ initially ordered by decreasing value of $p_{t_f(m)}(1,3)$ at our disposal. The time-average of the probability is computed using a Lyapunov method; this defines the permutation $I(\cdot)$ of $\{1,...,1000\}$ such that $I(m)$ is the rank of the controller $D(m)$ in the new classification by decreasing order of time-averaged probability; hence the controllers are reordered as $\{D(I(m))\}_{m=1}^{1000}$ by decreasing value of the time-averaged transfer probability they achieve. Naturally, as already observed from Fig. 4, one cannot expect complete consistency between the performance at the best time and the time-averaged performance. Nevertheless, despite this discrepancy, we show some unconventional behavior of the robust design $\mu_{\mathcal{D}}(G)$ versus the time-averaged performance. Traditionally, one would expect the robustness to deteriorate ($\mu \uparrow$) as the performance improves ($|\langle \mathrm{OUT}|\Psi\rangle| \uparrow$), but we show that around some controllers the reverse behavior happens.

To be somewhat more precise as to how the simulation was performed, we took an 11×11 Hamiltonian of the form (1) with $h_{1,11} = h_{11,1} = 1$. The P-matrix of Fig. 3 was taken as in Eq. (7). In this P-matrix, the output matrix C defining $z = C\Psi$ was taken as $C = \begin{pmatrix} e_1 & e_2 & 0_{11,1} & e_4 & \dots & e_{11} \end{pmatrix}^T$, where $\{e_k\}_{k=1}^{11}$ is the natural basis of $\mathbb{C}^{11}$ over $\mathbb{C}$ and $0_{11,1}$ is an 11-dimensional column vector with 0s everywhere; the matrix $S_{k,k+1}$ was taken as the 11×11 matrix with zeros everywhere except for 1's in positions $(5,6)$ and $(6,5)$; the matrix Φ was taken as $(sI + \imath H)_{s=0}^{-1} = (\imath H)^{-1}$. The G-matrix of Fig. 5 was computed as in Eq. (10). The $\mathcal{D}$ block structure was defined $\delta I_{11\times11} \oplus \mathbb{C}^{11\times11}$. The $\mu_{\mathcal{D}}(G)$ was computed using the `mussv` function of Matlab.

Note that the $|\mathrm{OUT}\rangle$ selectivity is picked up by the output z, but the analysis falls short of the $|\mathrm{IN}\rangle$ selectivity. The latter would require a Δ_p matrix structured as a single row in position corresponding to the $|\mathrm{IN}\rangle$ spin, but this appears beyond the capability of the `mussv` at this stage.

The results are summarized in Fig. 6. On the top panel, especially around controllers $I(m) \in [700, 850]$, one notices the unconventional behavior of decrease of the performance (fidelity $\downarrow$) concomitant with decrease of the robustness ($\mu \uparrow$). More precisely, it appears that the increase in μ follows the rate of decrease of the fidelity. A theoretical explanation of this latter phenomenon remains to be formulated, though. The bottom panel is essentially the same as the top, except for some rescaling, with the addition of the differential sensitivity as defined by Eq. (5). The unconventional behavior of the differential sensitivity versus the fidelity is quite obvious, but more importantly observe that the differential sensitivity has its "crossover" in the same interval, $I(m) \in [700, 850]$, as already singled out on the top panel.

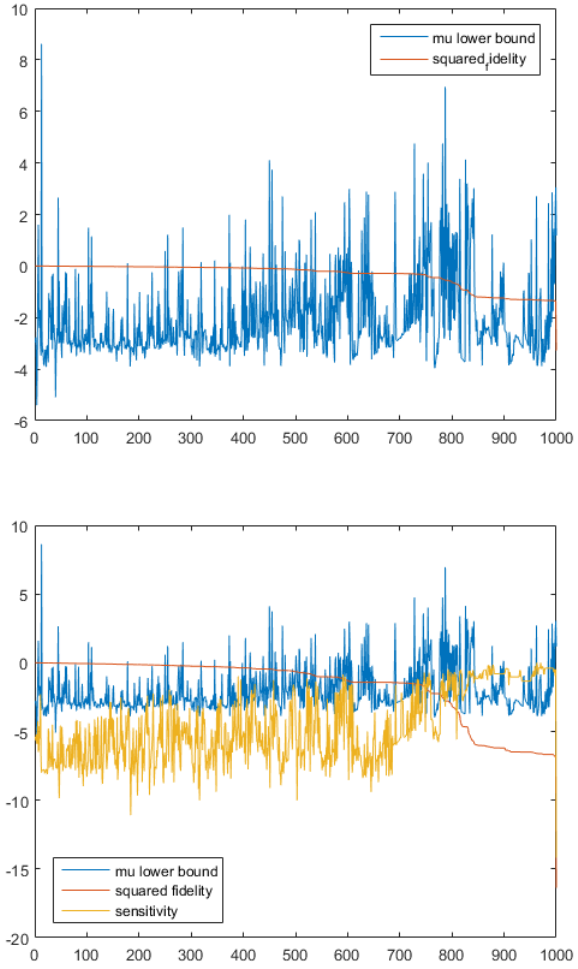

Fig. 6. Robust design μ, average fidelity, and differential sensitivity achieved by various controllers ordered by decreasing value of their average fidelity (bottom plot was rescaled for better visualization.)

All of the above qualitative observations can be confirmed by quantitative Kendall τ analysis. The visually obvious consistent behavior of the differential sensitivity and the μ is confirmed by a Kendall τ of 0.6672. The overall Kendall τ of the μ lower bound and the squared fidelity is -0.1601, indicating a slight negative correlation, as claimed. In the $I(m) \in [700, 850]$ area, this result can be improved by considering the *incremental* squared fidelity and μ, which negatively correlate with a Kendall τ of -0.1970.

VII. Conclusion

We have shown that the reassuring good sensitivity properties of high fidelity excitation transport controllers for spintronic networks demonstrated in [15], [23] can be extended to larger variation, so that such controllers can be objectively referred to as "robust." Both classical differential sensitivity and μ analyses reveal a nonclassical crossover region in the space of controllers where fidelity, classical sensitivity, and robustness as quantified by the μ-function all deteriorate—a rather surprising observation that contradicts the classical limitations on achievable performance. This quantum-classical

discrepancy can be explained by the field-mediation of the quantum control while classical control is measurement-mediated.

It is still technologically challenging to address the individual spins of the network with well focused magnetic fields. This is the reason why sensitivity against field focusing errors was considered in [23] and shown to vanish for perfect state transfer controllers. This technological difficulty could be overcome on a theoretical basis by addressing "islands" of spins instead of single spins using multiple excitation [22] and possibly next nearest neighbor couplings [18]. This is left for further research. A more technically viable solution is provided by ultracold atom quantum simulators [3], where laser pulses can address single atoms and the energy landscape can be controlled, as it is here. More specifically, Heisenberg chain simulators based on optical lattices [10], atom cavities [4], trapped ions [8] offer plenty of techniques for energy landscape shaping and single atom pseudo-spin addressing that reproduce the theoretical model adopted here (with a preference for cavity models where single atom addressing seems easier [4]). Furthermore, some copper compounds [21] nearly reproduce the theoretical behavior of the 1-dimensional chains considered here.

We have chosen controllers that transport the excitation in a minimum amount of time [20] to mitigate decoherence. Conceptually, the approach proposed here can easily be extended to networks subject to decoherence by replacing Schrödinger's equation with von Neumann-Lindblad's equation, but at the expense of a serious curse of dimensionality, as the original N-dimensional problem now becomes a N^2-dimensional problem. This is left for further research.

REFERENCES

[1] P. W. Anderson. Absence of diffusion in certain random lattices. *Physical Review*, 109(5):1492–1505, March 1958.

[2] V. Belevitch. *Classical Network Theory*. Holden-Day, San Francisco, 1968.

[3] Immanuel Bloch, Jean Dalibard, and Sylvain Nascimbène. Quantum simulations with ultracold quantum gases. *Nature Physics*, 8:267276, 2012.

[4] Z.-X Chen, Z.-W Zhou, X. Zhou, X.-F Zhou, and G.-C. Guo. Quantum simulation of Heisenberg spin chains with next nearest neighbor interactions in coupled cavities. *Phys. Rev. A*, 81:022303, 2010. arXiv:1212.5328v1 [quant=ph] 21 Dec 2012.

[5] W. B. Dong, R.-B.Wu, W. Zhang, C. W. Li, and T. J. Tarn. Spatial control model and analysis of quantum fields in one-dimensional waveguides. *SIAM Journal on Control and Optimization*, 54(3):1352–1377, 2016.

[6] D. D. Awschalom *et al.* Quantum spintronics: Engineering and manipulating atom-like spins in semiconductors. *Science*, 339(6124):1174–1179, March 2013.

[7] S. A. Wolf *et al.* Spintronics: A spin-based electronics vision for the future. *Science*, 294(5546):1488–1495, November 2001.

[8] T. Grass and M. Lewenstein. Trapped-ion quantum simulation of tunable-range Heisenberg chains. *EPJ Quantum Technology*, 1:8, 2014. doi:10.1140/epjqt8.

[9] Dirk Hundertmark. A short introduction to Anderson localization. In *Proceedings of the LMS Meeting on Analysis and Stochastics of Growth Processes and Interface Models*, pages 194–218. Oxford University Press, Oxford, United Kingdom, 2008.

[10] C.-L. Hung, A. Gonzales-Tudela, J. Ignacio Cirac, and H. J. Kimble. Quantum spin dynamics with paiwise-tunable, long-range interactions. *PNAS*, pages E4946–E4955, August 2016.

[11] E. Jonckheere, F. C. Langbein, and S. G. Schirmer. Curvature of quantum rings. In *Proceedings of the 5th International Symposium on Communications, Control and Signal Processing (ISCCSP 2012)*, Rome, Italy, May 2-4 2012. DOI: 10.1109/ISCCSP.2012.6217863.

[12] E. Jonckheere, S. Schirmer, and F. Langbein. Geometry and curvature of spin networks. In *IEEE Multi-Conference on Systems and Control*, pages 786–791, Denver, CO, September 2011. DOI: 10.1109/CCA.2011.6044395. Available at arXiv:1102.3208v1 [quant-ph].

[13] E. Jonckheere, S. Schirmer, and F. Langbein. Quantum networks: The anti-core of spin chains. *Quantum Information Processing*, 13:1607–1637, 2014. Published on line May 24, 2014. (DOI: 10.1007/s11128-014-0755-5). Available at `http://eudoxus2.usc.edu`.

[14] E. Jonckheere, S. Schirmer, and F. Langbein. Information transfer fidelity in spin networks and ring-based quantum routers. *Quantum Information Processing (QINP)*, 14(10), 2015. DOI: 10.1007/s11128-015-1136-4; available at `http://eudoxus2.usc.edu` and arXiv:submit/1359959 [quant-ph] 24 Sep 2015.

[15] E. Jonckheere, S. Schirmer, and F. Langbein. Jonckheere-Terpstra test for nonclassical error versus log-sensitivity relationship of quantum spin network controllers. *International Journal of Robust and Nonlinear Control*, 2016. Submitted, available at arXiv:1612.02784 [math.OC].

[16] E. A. Jonckheere and Nainn-Ping Ke. Complex-analytic theory of the μ-function. *Journal of Mathematical Analysis and its Applications*, 237:201–239, 1999.

[17] E. A. Jonckheere and Nainn-Ping Ke. Real versus complex robustness margin continuity as a smooth versus holomorphic singularity problem. *Journal of Mathematical Analysis and its Applications*, 237:541–572, 1999.

[18] L. C. Kweck, Y. Takahashi, and K. W. Choo. Spin chain under next nearest neighbor interaction. *Journal of Physics: Conference Series*, 143, 2009. doi: 10.1088/1742-6596/143/1/012014.

[19] A. Lagendijk, B. van Tiggelen, and D. Wiersma. Fifty years of Anderson localization. *Physics Today*, 62:24–28, August 2009.

[20] F. Langbein, S. Schirmer, and E. Jonckheere. Time optimal information transfer in spintronics networks. In *IEEE Conference on Decision and Control*, pages 6454–6459, Osaka, Japan, December 2015.

[21] J. M. Maillet. Heisenberg spin chains: from quantum groups to neutron scattering experiments. *Séminaire Poincaré*, X:129–177, 2007.

[22] T. Orsborne. Static and dynamic of quantum XY and Heisenberg systems on graphs. arXiv: quant-ph/0312126v3, 2006.

[23] S. Schirmer, E. Jonckheere, and F. Langbein. Design of feedback control laws for spintronics networks. *IEEE Transactions on Automatic Control*, 2016. Under revisions; available at arXiv:1607.05294.

[24] K. Zhou and J. C. Doyle. *Essentials of robust control*. Prentice Hall, Upper Saddle River, NJ, 1998.